Neuropsychiatric Disease and Treatment

Dovepress

open access to scientific and medical research

Open Access Full Text Article

ORIGINAL RESEARCH

Computed Tomography, Magnetic Resonance Imaging, and Pathological Features of Gliosarcoma

Haiqing Fan*, Yue Yu*, Jinhui Du, Likun Liu, Yilin Luo, Hui Yu, Xin Liao

Department of Medical Imaging, The Affiliated Hospital of Guizhou Medical University, Guiyang City, Guizhou Province, 550004, People's Republic of China

*These authors contributed equally to this work

Correspondence: Xin Liao, Department of Medical Imaging, The Affiliated Hospital of Guizhou Medical University, No. 29 Guiyi Street, Yunyan District, Guiyang City, Guizhou Province, 550004, People's Republic of China, Tel +86 13765065226, Email liaoxinlxlx@126.com

Objective: To investigate the clinical, imaging, and pathological features of gliosarcoma.

Methods: The clinical data of 14 patients with gliosarcoma confirmed by surgery and pathology at our hospital between 2010 and 2021 were analyzed retrospectively, and the relevant literature was reviewed.

Results: In all 14 cases, the gliosarcoma was located in the supratentorial brain parenchyma and involved a single lesion. There were more male patients (64.3%) than female patients (35.7%), and 57.1% of all the patients were 40–60 years of age. The prognosis of all 14 patients was poor, and the average survival time was approximately seven months. The computed tomography findings revealed mostly mixed density lesions, and some cases were complicated with bleeding. The magnetic resonance imaging revealed irregularly shaped mass lesions of different sizes, with uneven or circular enhancement. Cystic degeneration and necrosis could be seen in all the masses, some of which showed signs of bleeding and were surrounded by different degrees of edema and space-occupying effects. The pathological examination revealed that the tumors had bidirectional differentiation of the glial and sarcoma components, while the immunohistochemistry examination revealed glial fibrillary acidic protein-positive and reticular fiber-positive staining in the sarcoma.

Conclusion: The clinical manifestations of gliosarcoma are nonspecific, but imaging reveals that the condition has certain characteristics, typically consisting of a huge supratentorial mass, with an irregular heterogeneous periphery or obvious mass-like augmentation after enhancement. The final diagnosis depends on the results of a pathological examination.

Keywords: brain, gliosarcoma, computed tomography, magnetic resonance imaging, pathology

Introduction

Gliosarcoma is a subtype of glioblastoma with mesenchymal differentiation, and it is classified as a grade IV tumor by the World Health Organization.[1] The condition has the histological characteristics of glioblastoma and soft-tissue sarcoma[2] and is clinically rare. The current treatment is similar to that used for glioblastoma and is primarily surgical, supplemented with postoperative radiotherapy and chemotherapy.[3,4] The prognosis is extremely poor, even after standardized treatment, and the mean overall survival time is only 6.6–18.5 months.[5] The condition also has a high rate of recurrence and metastasis.

Computed tomography (CT) and magnetic resonance imaging (MRI) are conducive to revealing the positioning and the qualitative diagnosis of the lesions, and they present important methods for the examination of tumor lesions in the central nervous system. However, gliosarcoma has similar imaging manifestations to glioblastoma,[6] meaning the accuracy of the imaging for preoperative diagnosis is generally low.

A total of 14 cases of gliosarcoma that were confirmed postoperatively via pathological examination at our hospital were analyzed retrospectively, with the CT and MRI findings and the pathological features analyzed, while the relevant literature was also reviewed and summarized to enhance the understanding of the disease.

Received: 17 August 2022
Accepted: 14 October 2022
Published: 4 November 2022

Clinical Data

General Information

The data relating to 14 cases of gliosarcoma confirmed via surgery and pathological examinations at our hospital between January 2010 and October 2021 were collected. The patients included nine males and five females aged 23–70 years (median = 54 years), with 12 patients aged under 40.

Location of Lesion and Clinical Manifestations

The location, size, and shape of the lesions varied across the 14 cases of gliosarcoma. The vast majority of the patients had a short onset time, and the clinical manifestations were nonspecific, with the main manifestations being headache, dizziness, nausea, vomiting, weakness in the limbs inducing an unsteady gait, and changes in visual acuity and mental state (Table 1). Headache (eight cases), dizziness (six cases), and weakness in the limbs (six cases) were the most common symptoms (Table 2). The symptoms had lasted for around one year at most, with the shortest symptom duration around five days. Meanwhile, 13 cases involved the first episode of gliosarcoma, while one case involved recurrence of the condition three months after the initial surgery (pathologically confirmed as gliosarcoma after the second operation),

Table 1 Clinical Data of 14 Patients with Gliosarcoma

Clinical Characteristics (n)	Number of Cases (n=14)	Percentage (%)
Gender (case)		
Male	9	64
Female	5	36
Age (n)		
<40 years old	2	14
>40 years old	12	86
Chief complaint (n)		
Neurological symptoms	14	100
Abnormal limb activities	6	43
Gastrointestinal symptoms	3	21
Cerebral hemisphere site (cases)		
Left side		
Frontal lobe	2	14
Temporal lobe	2	14
Occipital lobe	1	7
Right side		
Frontal lobe	1	7
Frontal temporal lobe	3	21
Frontal parietal lobe	1	7
Temporal lobe	2	14
Temporal parietal lobe	1	7
Parietal occipital lobe	1	7

Table 2 Neurological Symptoms of 14 Patients with Gliosarcoma

Neurological Symptoms (n)	Number of Cases (n=14)	Percentage(%)
Headache	8	57
Dizziness	6	43
Weakness of the limbs	6	43
Unstable walking	1	7
Limb activity disorder	1	7
Vision change	3	21
Changes in mental state	2	14

with a history of radiotherapy and chemotherapy. These 14 cases of gliosarcoma accounted for 1.3% of all glioblastoma cases treated at the hospital in the same period (Table 3).

Imaging Data

Scanning Methods

A Siemens Somatom Sensation 16 CT scanner and a GE Signa 1.5T superconducting magnetic resonance scanner head coil were used for the scanning. Six patients underwent a non-enhanced CT scan, with a 5-mm scanning slice thickness and a 3-mm interslice gap. All 14 patients underwent non-enhanced and enhanced MRI scanning, using axial T_1-weighted imaging (T_1WI), T_2WI, T_2/fluid-attenuated inversion recovery (FLAIR), diffusion weighted imaging (DWI), and sagittal T_2WI and spin echo sequences. The T_1WI repetition time (TR) was 500 ms and the echo time (TE) was 25 ms, while the T_2WI TR was 5000 ms and the TE was 106 ms. The field of view (FOV) was 24×24 cm, the slice thickness was 5 mm, the interslice gap was 2 mm, and the matrices were 256–512 × 256–512. At the time of the enhanced scanning, gadolinium diethylenetriaminepentaacetic acid was injected intravenously into the elbow at a dose of 0.1 mmol/kg body weight, and T_1WI axial, coronal, and sagittal sequences were used for the scanning. In four cases, magnetic resonance spectroscopy (MRS) was performed using a multivoxel point-resolved spectroscopy sequence, with a TE of 144 ms. The regions of interest included the solid and cystic parts of the mass and the contralateral normal brain parenchyma. In four cases, diffusion tensor imaging (DTI) was performed using an echo planar imaging sequence. For the MRS and the DTI, the FOV was 24×24 cm, and the b values were 0 and 1000 s/mm^2, respectively.

Image Analysis

All the images were read by two diagnostic imaging radiologists with senior professional titles, using the blind method. The following were analyzed: the location, size, shape, and boundaries of the masses; the degree of edema; the space-occupying effect; the density and signal characteristics; the presence of cystic necrosis and hemorrhaging; and the enhancement. The evaluations that were consistent were regarded as the final diagnostic results.

Pathological Examination

A total of 14 tumor specimens were surgically removed, fixed with 10% formalin, routinely dehydrated, waxed, and embedded with paraffin before being consecutively sliced into sections that were used for hematoxylin and eosin, immunohistochemical, and reticular fiber staining.

Table 3 Treatment and Prognosis of 14 Patients with Gliosarcoma

Case (n=14)	Gender	Age	Operation Mode	Postoperative Radiotherapy and Chemotherapy	Overall Survival
1	Male	23	Total tumor resection	Radiotherapy and chemotherapy	8 months
2	Male	43	Subtotal tumor resection	Radiotherapy and chemotherapy	6 months
3	Male	44	Subtotal tumor resection	Radiotherapy and chemotherapy	6 months
4	Male	44	Total tumor resection	Radiotherapy and chemotherapy	In follow-up
5	Male	53	Subtotal tumor resection	Radiotherapy and chemotherapy	10 months
6	Male	58	Subtotal tumor resection	Chemotherapy	1 month
7	Male	68	Total tumor resection	None	In follow-up
8	Male	68	Subtotal tumor resection	None	4 months
9	Male	70	Subtotal tumor resection	None	4 months
10	Female	25	Total tumor resection	Radiotherapy and chemotherapy	In follow-up
11	Female	44	Subtotal tumor resection	Radiotherapy and chemotherapy	14 months (recurrence postoperatively after 12 months)
12	Female	54	Subtotal tumor resection	Radiotherapy and chemotherapy	8 months
13	Female	62	Subtotal tumor resection	Radiotherapy and chemotherapy	6 months (recurrence postoperatively after 3 months)
14	Female	70	Subtotal tumor resection	None	Died of respiratory failure after surgery

Results

Lesion Location, Size, and Shape

All 14 cases presented with a single supratentorial lesion, with three in the frontal lobe, four in the temporal lobe, one in the occipital lobe, three in the frontal and temporal lobes, one in the frontal and parietal lobes, one in the temporal and parietal lobes, and one in the parietal and occipital lobes. In one case, the tumor protruded into the lateral ventricle, in another, the tumor involved the corpus callosum, and, in two cases, the tumor invaded the adjacent meninges.

The largest mass was approximately 6.4×6.6 × 7.7 cm, and the smallest was approximately 2.7×4.8 × 3.5 cm. The shapes were irregular, the boundaries were unclear, and the tumors exhibited varying degrees of space-occupying effect. Three cases had obvious deviation of the midline structure to the opposite side, and one case had hydrocephalous. In 10 cases, there was obvious hydrocephalous edema, and, in four cases, there was mild edema around the tumor masses (see Table 4).

Computed Tomography Findings

Non-enhanced CT scanning was performed on six patients, revealing isodense or slightly dense masses of uneven density. The CT Hounsfield unit (HU) value was 22–60, but there were necrotic areas and areas with cystic degeneration in which the CT HU value was 0–22. High-density hemorrhaging was found in three other cases, in which the CT HU value was approximately 63 (Figure 1). None of the patients underwent an enhanced CT examination (Table 4).

Magnetic Resonance Imaging Manifestations

All the patients underwent non-enhanced and enhanced MRI scanning. The signals of all the masses were mixed; the T_1WI and T_2WI sequences exhibited mainly isointense and hypointense signals (Figure 2). In terms of the DWI images, the masses presented with restricted diffusion, while the T_2/FLAIR images revealed that the masses exhibited mixed signals (Figures 3 and 4). Cystic degeneration and necrosis could be seen in all the masses. In four cases, the cystic degeneration was giant and located at the edge of the mass, and bleeding was found in the masses of four cases.

Enhanced MRI scanning revealed that the masses were significantly and unevenly enhanced, but that there was no enhancement in the area of cystic degeneration and necrosis. There was irregular ring enhancement in seven cases, where

Table 4 Imaging Manifestations of 14 Patients with Gliosarcoma

Case (n=14)	Gender	Age	Imaging Manifestations
1	Male	23	CT: mixed dense mass with hemorrhage MRI: irregular ring-enhancement, with giant cystic degeneration
2	Male	43	MRI: mass-like uneven enhancement, protruded into the lateral ventricle
3	Male	44	MRI: irregular ring-enhancement, with obvious surrounding edema
4	Male	44	CT: mixed dense mass with hemorrhage MRI: irregular ring-enhancement, with giant cystic degeneration
5	Male	53	CT: mixed dense mass MRI: mass-like uneven enhancement
6	Male	58	MRI: irregular ring-enhancement, with cystic degeneration and obvious surrounding edema
7	Male	68	MRI: mass-like uneven enhancement
8	Male	68	CT: mixed dense mass MRI: irregular ring-enhancement, with obvious surrounding edema
9	Male	70	CT: mixed dense mass MRI: mass-like uneven enhancement
10	Female	25	CT: mixed dense mass with hemorrhage MRI: mass-like uneven enhancement
11	Female	44	MRI: mass-like uneven enhancement, with obvious surrounding edema
12	Female	54	MRI: irregular ring-enhancement, with obvious surrounding edema
13	Female	62	MRI: irregular ring-enhancement, with giant cystic degeneration
14	Female	70	MRI: irregular ring-enhancement, with giant cystic degeneration

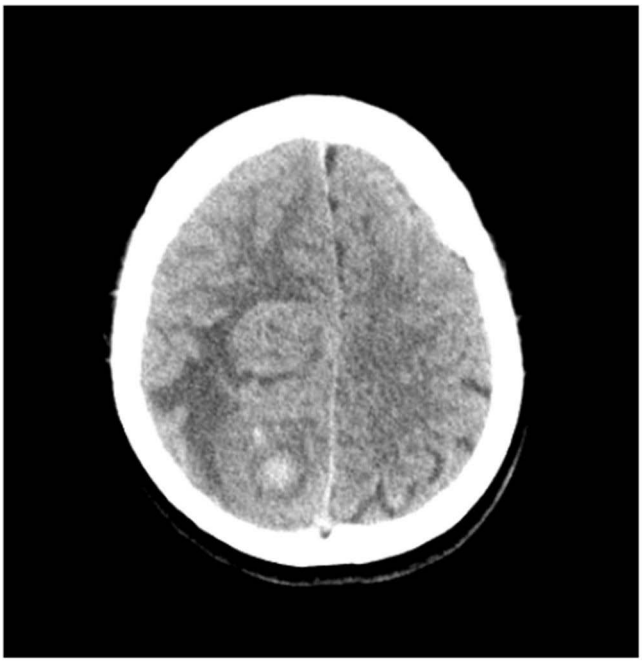

Figure 1 Female (25 years old) with headache and left lower limb weakness for two months. Computed tomography plain scan showing a mixed mass with high density hemorrhage in the right frontal and parietal lobes.

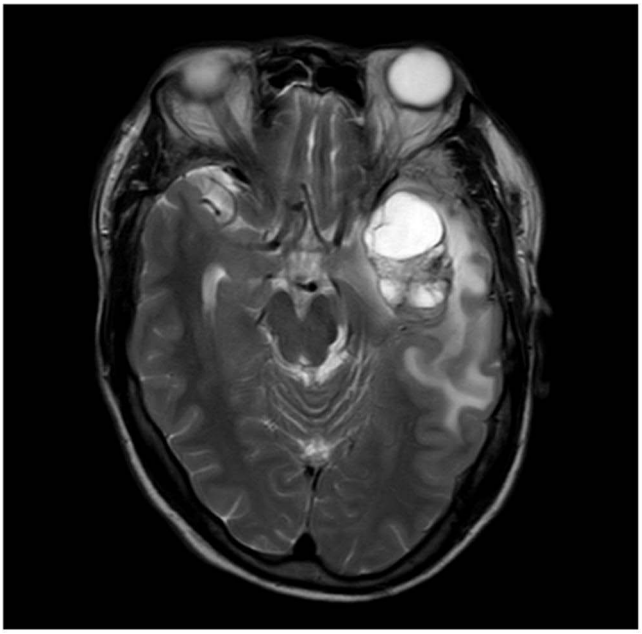

Figure 2 Male (44 years old) with headache and blurred vision for one month. T_2WI showing the internal hemorrhage of the mass with high signal intensity and perilesional edema/infiltration.

the cystic walls of giant cystic degeneration were enhanced, and there was mass-like obvious enhancement in the other seven cases (Figure 5). Four patients underwent MRS examination, and the peak value of choline (Cho) increased significantly. The peak value of N-acetylaspartate (NAA) and creatine (Cr) decreased, manifesting as a significant increase in the Cho/Cr ratio and Cho/NAA ratio and a decrease in the NAA/Cr ratio (Figures 6 and 7). Lactate (Lac) and

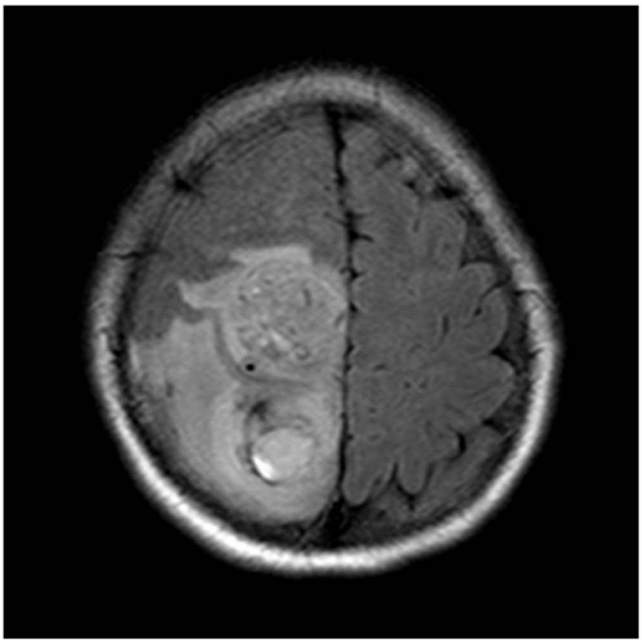

Figure 3 Female (25 years old) with headache and left lower limb weakness for two months. T_2/fluid-attenuated inversion recovery showing internal hemorrhaging of the mass with a slightly higher signal intensity and obvious edema around it.

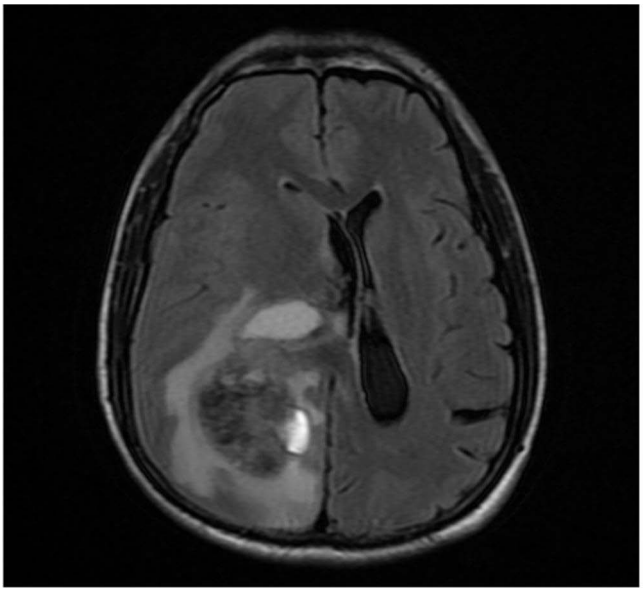

Figure 4 Male (43 years old) with headache and dizziness for six months. T_2/fluid-attenuated inversion recovery showing the internal signal intensity of the mass is clear, and the edema is obvious around the mass.

lipid (Lip) peaks were revealed in the MRS of two patients. Four patients had a DTI scan in which it was clear that the white matter fiber bundle in the mass area was amputated and reduced (Figure 8).

Pathological and Immunohistochemical Results

Generally, the tumors were tough, and the sections were gray, grayish yellow, or grayish brown. On microscopic examination, it was observed that the tumor cells were composed of differently proportioned glial and sarcoma

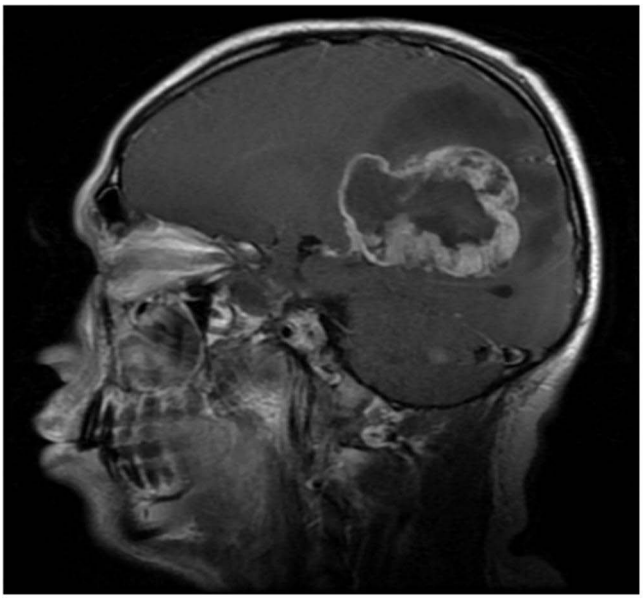

Figure 5 Male (43 years old) with headache and dizziness for six months. T_1WI enhancement showing tumors exhibiting irregular ring enhancement, some with thicker walls and wall nodules.

Figure 6 Female (25 years old) with headache and left lower limb weakness for two months. Magnetic resonance spectroscopy showing the internal choline peak of the tumor was significantly increased, creatinine peak was decreased, and the N-acetylaspartate peak was obviously decreased.

Figure 7 Male (68 years old) with dizziness for twenty days. Magnetic resonance spectroscopy showing the internal choline peak of the tumor was significantly increased, creatinine peak was obviously decreased, and the N-acetylaspartate peak was decreased.

components. The tumor cells grew diffusely with vascular proliferation, and there were abundant reticular fibers among them. There were also large areas of coagulative necrosis and vascular hyaline degeneration. The immunohistochemical analysis was positive for both glial fibrillary acidic protein (GFAP) and vimentin, and it revealed that the Ki-67 expression level of two types of lesions was >10% and that the staining of the reticular fibers was positive for all the tumors. The immunohistochemical analysis was also positive for isocitrate dehydrogenase 1, O-6-methylguanine-DNA methyltransferase, and P53 in a number of tumors.

Treatment and Prognosis

The vast majority of the 14 patients had clinical symptoms for the first time within the month before they were treated. All of them were given surgical treatment, one patient received postoperative chemotherapy, and nine patients received postoperative chemotherapy and radiotherapy. One patient died of respiratory failure after exhibiting unstable vital signs in the postoperative period, and 10 patients experienced recurrence postoperatively, the shortest recurrence time being 1 month and the longest 14 months (average = 7 months). One of the 14 patients had cerebrospinal fluid seeding and distant metastasis at the same time (Table 3).

Discussion

Clinical Characteristics

The term “gliosarcoma” was first introduced by Stroebe in 1895,[7] and the condition accounts for approximately 2–8% of glioblastomas.[8] The mechanism of the tumor is not only related to genetic factors, and researchers have considered that glioblastoma may be primary and sarcoma secondary.[9] This could explain why, in this study, one patient was initially diagnosed with glioblastoma via postoperative pathology, but when the tumor recurred three months later, it was diagnosed via postoperative pathology as gliosarcoma. It has been found that people aged 40–60 have a high prevalence of tumors, with a male to female ratio of 1.75:1.[10] Gliosarcoma in children is very rare, while its

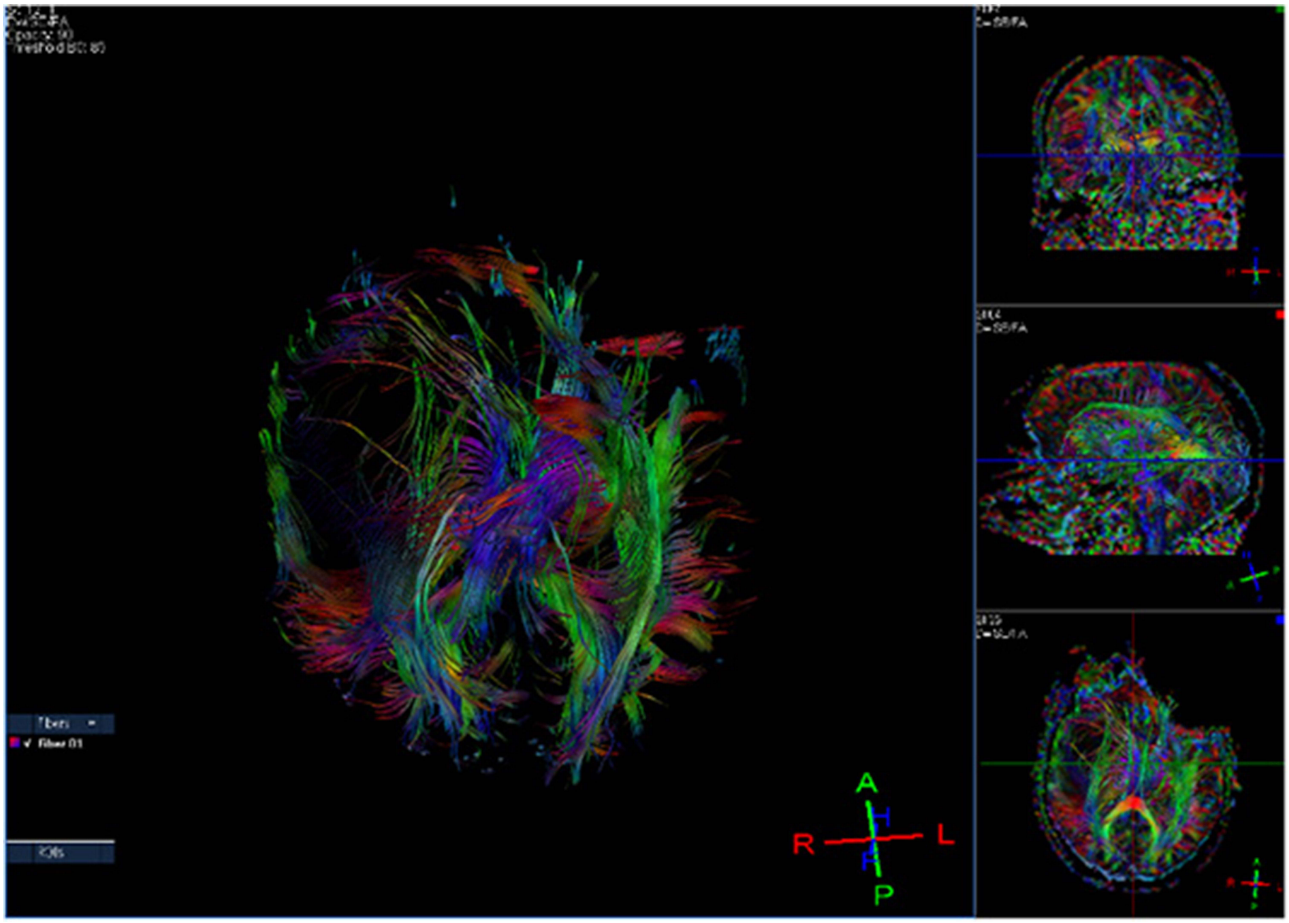

Figure 8 Male (58 years old) with headache, dizziness, and fatigue for seven days. Diffusion tensor imaging showing the white mass fiber bundle in the mass area was significantly interrupted and reduced.

clinicopathological features and prognosis are similar to those in adults.[11] The cerebral hemisphere is the most common site for the disease, and the tumor most often occurs in the temporal lobe (followed by the frontal and parietal lobes), which may be due to the greater sensitivity of the temporal lobe to tumors compared with the other lobes.[5,8,10] Gliosarcoma is rarest in the infratentorial region of the brain, the ventricles, the pineal gland, and the optic nerve.[12–15] Most cases present with a single mass, and multiple masses are rarely reported.[16,17] Gliosarcoma often grows across the brain lobes, and it generally has a large volume and an obvious space-occupying effect and can easily invade the adjacent meninges.[18]

This study included nine males and five females, with a male to female ratio of 1.8:1, and 40–60-year-old accounted for 57.1% of the study subjects. The tumors affected the temporal lobe in eight cases and the frontal lobe in seven, while they invaded the adjacent meninges in two, which is consistent with the incidence of gliosarcoma reported in the literature. Patients with gliosarcoma most commonly present with symptoms related to increased intracranial pressure, such as headache, nausea, vomiting, and decreased vision, as well as signs of focal neurological deficits caused by tumor compression, such as limb fatigue and numbness. All these symptoms were reported in this study.

The incidence of extracranial metastases of gliosarcoma is approximately 11%.[19] The most common sites of extracranial metastasis reported in the literature are the lung, the liver, and the lymph nodes.[20] The occurrence of metastases may be related to the dedifferentiation of sarcoma and the destruction of the normal anatomical barrier during surgical resection.[21]

Imaging Features

Brain tumors are generally detected via cranial CT and MRI.[22] The latter is generally considered superior to the former, since it can display the location, size, shape, boundary, density, and signal and enhancement characteristics of any lesions.[22] The imaging findings are closely related to pathological changes. On non-enhanced CT scans, the gliosarcoma presents primarily as isointense and hypointense mixed density masses, while a few tumor masses may be slightly hyperintense. However, some can present as tumors with unclear boundaries and irregular shapes, cystic degeneration, necrosis, and bleeding. On an enhanced CT scan, the gliosarcoma exhibits even enhancement (primarily peripheric enhancement), with the solid part of the tumor clearly enhanced, enhancement in the cystic wall, and no enhancement in the areas of cystic degeneration and necrosis.[23]

In this study, on the non-enhanced CT scans, six patients had masses of mixed density with areas of hypointense cystic degeneration and necrosis, three patients had masses with high-density hemorrhaging, one patient had a mass that protruded into the lateral ventricle, and one patient had a mass that involved the corpus callosum.

The non-enhanced MRI scans revealed that the masses had irregular abnormal signals, and a hyperintense signal was observed when bleeding was found. The T_2WI sequences exhibited unevenly mixed isointensity and hyperintensity, and the internal capsule degeneration and necrosis exhibited a high signal.[24]

In terms of the DWI images, the diffusion of the solid part was restricted, but the diffusion of the cystic degeneration and necrosis was unrestricted, and T_2/FLAIR was sensitive to edema around the mass. The enhanced MRI scanning revealed significant uneven enhancement and extremely irregular shapes in the masses. There were two different manifestations of enhancement. Peripheric enhancement is common due to cystic degeneration, necrosis, and bleeding, and enhancement can be seen in the cystic wall. This was observed in one case. In another case, there was relatively little cystic degeneration and necrosis in the mass, which enhanced the shape of the mass, with uneven enhancement inside. The edema around the mass exhibited no enhancement, and the invaded adjacent meninges exhibited clear linear enhancement.[23,25] In this study, all 14 patients underwent non-enhanced MRI scanning and enhanced MRI scanning, and the morphological changes, signal characteristics, and edema of the masses were consistent with those reported in the literature. Seven cases exhibited irregular annular enhancement and enhancement in the cystic wall of giant cystic degeneration, seven cases had clear mass enhancement, and two cases had clear enhancement of the invaded meninges. Four patients underwent an MRS scan, which revealed that the Cho peaks in the masses was significantly increased, and the NAA peaks in the masses and around the area of the edema were significantly decreased. Four patients underwent DTI, and the results revealed that there was destruction of the white matter fiber bundles in the area of the mass, suggesting that the destruction of neurons by a tumor is closely related to the proliferation of glial fibers and reflects the growth mode of the malignant infiltration of the tumor.

Diagnosis and Pathological Characteristics

Pathologically, the biphasic differentiation into glial and mesenchymal tissues is the key to the diagnosis of gliosarcoma. The glial component exhibits typical characteristics of glioblasts, with varying degrees of anaplasia and GFAP expression. Sarcoma areas often show long dense spindle cells, arranged in a fishbone fibrosarcoma structure. The sarcoma component may have malignant characteristics, such as an atypical nucleus, active mitosis, and necrosis. Due to the formation of reticular fibers, the sarcoma area is clearly distinguishable from the glioma. For diagnostic purposes, it is crucial to identify reticular fibers in sarcomas and GFAP in glioma components. Specifically, sarcomas have rich reticular fibers and are negative for GFAP, while the glial components lack reticular fibers and are positive for GFAP.[4,11,26,27] Gliosarcoma can also present with other types of mesenchymal differentiation, such as smooth and striated muscle, lipoma, and primitive nerve differentiation and differentiation in bone and cartilage formation.[11] In some cases, epithelial metaplasia, with keratinized stratified epithelial cells and gland formation, has been found. In this study, clear cystic degeneration and necrotic areas were seen in all the cases, and a few bleeding foci were seen in some of them. At present, the diagnosis of gliosarcoma still depends on postoperative pathology and immunohistochemistry examinations.

Differential Diagnoses

Gliosarcoma and glioblastoma are difficult to distinguish, and the final diagnosis depends on a pathological examination. Gliosarcoma exhibits irregular ring-enhancement on enhanced scanning, which needs to be differentiated from an intracranial metastatic lesion or a brain abscess. The ring walls of the latter two are regular, and these two diseases can be distinguished by combining the results of clinical history, DWI, MRS, and other tests. One study aimed to differentiate primary and secondary malignant tumors of the central nervous system, based on single-voxel short TE and multi-voxel long TE proton MRS. The results indicated that there was a good correlation between the NAA/Cr and Cho/Cr ratios, which was more obvious in metastatic tumors. The NAA/Cr value of a metastatic tumor is higher than that of high-grade glioma, and the Lac/Cr value is significantly lower than that of glioma and primary central nervous system lymphoma, while the Lip and Lac peaks of gliosarcoma, metastatic tumors, and some high-grade gliomas are similar. It is generally believed that due to ischemia following cell injury, lactic acid production increases, and with the progress of the injury, there will be a Lip peak. The Lip peak in the solid component is related to the mesenchymal component (rather than the glial component) of gliosarcoma, the fat component of a metastatic tumor, tumor necrosis, and a poor prognosis. In addition, as a non-invasive method of evaluating brain tissue metabolism, spectral analysis can be used to differentiate high- and low-grade gliomas. Analysis has revealed that there may be similarities between the metabolite levels of different grade gliomas; for example, the rise in creatine may be similar, while the level of creatine in metastatic tumors may be lower.[28–30]

Gliosarcoma can also be differentiated from lymphoma since the signals they produce in plain and enhanced scans differ, and circular enhancement is rare for lymphoma. Lymphoma predominantly exhibits hypointensity or isointensity on T_1WI and T_2WI, and clear and intense enhancement can be observed following contrasting. However, when there are many liquefied and necrotic components, lesions exhibit a hypointense signal on T_1WI and a hyperintense signal on T_2 WI. Correspondingly, there is peripheric enhancement following contrasting.[31]

Treatment and Prognosis

Gliosarcoma is a highly rare malignant tumor of the central nervous system, which progresses rapidly and relapses and metastasizes easily, and its prognosis is poor.[20,32,33] At present, surgery is the primary treatment, supplemented with radiotherapy and chemotherapy, and without treatment, the average survival time is four months.[34] Most tumor recurrence is also gliosarcoma, while there have been a few reports of glioblastoma.[35] The patients with large cystic changes, hemorrhaging, or both, in the 14 cases in this study, had a higher rate of incomplete resection and only received postoperative chemotherapy or no therapy at all, and the patients who had a complete resection lived for longer.

Limitations

As a single-center retrospective analysis, this study had certain limitations. First of all, most of the 14 patients only underwent plain CT and MRI scans and an enhanced MRI scan. Only four patients underwent MRS, and only four patients underwent DTI. This was because, at that time, CT/MR perfusion imaging and other examination techniques were not available. Secondly, the survival period of the 14 patients was short, meaning only one patient had cerebrospinal fluid metastases. Finally, only the main nervous system symptoms of the patients were investigated. Future studies could expand the sample size, conduct a multi-center retrospective analysis, use more advanced technology, and ensure regular and frequent follow-ups.

Outlook

At present, the question of how to diagnose gliosarcoma efficiently, accurately, and at an early stage without solely relying on a pathological examination is critical to the effectiveness of follow-up treatment and the long-term prognosis of the patients. In recent years, radiomics, which primarily relies on the collection of imaging data, the segmentation of regions of interest, image feature extraction and feature analysis, as well as the creation of predictive models, has been widely used in the diagnosis of central nervous system tumors.[36] Researchers have also established a predictive model

based on radiomics to distinguish patients with glioblastoma from those with glioma, and the predictive value of the model is good.[6] In the future, radiomics and machine learning methods could be used for more in-depth research to improve the accuracy of the preoperative differentiation of glioblastoma and gliosarcoma.

Abbreviations

CT, Computed tomography; MRI, magnetic resonance imaging; FLAIR, fluid-attenuated inversion recovery; TR, repetition time; TE, echo time; FOV, field of view; MRS, Magnetic resonance spectroscopy; DTI, Diffusion tensor imaging; NAA, N-acetylaspartate; GFAP, glial fibrillary acidic protein.

Ethical Statement

This study was conducted with approval from the Ethics Committee of The Affiliated Hospital of Guizhou Medical University. This study was conducted in accordance with the declaration of Helsinki. Written informed consent was obtained from all participants.

Funding

National Natural Science Foundation of China (No. 81960537).

Disclosure

The authors report no conflicts of interest in this work.

References

1. Dardis C, Donner D, Sanai N, et al. Gliosarcoma vs. glioblastoma: a retrospective case series using molecular profiling [published correction appears in BMC Neurol. 2021 Aug 14; 2 1):316]. *BMC Neurol*. 2021;21(1):231. doi:10.1186/s12883-021-02233-5
2. Zaki MM, Mashouf LA, Woodward E, et al. Genomic landscape of gliosarcoma: distinguishing features and targetable alterations. *Sci Rep*. 2021;11 (1):18009. doi:10.1038/s41598-021-97454-6
3. Frandsen J, Orton A, Jensen R, et al. Patterns of care and outcomes in gliosarcoma: an analysis of the National Cancer Database. *J Neurosurg*. 2018;128(4):1133–1138. doi:10.3171/2016.12.JNS162291
4. Yi X, Cao H, Tang H, et al. Gliosarcoma: a clinical and radiological analysis of 48 cases. *Eur Radiol*. 2019;29(1):429–438. doi:10.1007/s00330-018-5398-y
5. Feng SS, Li HB, Fan F, et al. Clinical characteristics and disease-specific prognostic nomogram for primary gliosarcoma: a SEER population-based analysis. *Sci Rep*. 2019;9(1):10744. doi:10.1038/s41598-019-47211-7
6. Qian Z, Zhang L, Hu J, et al. Machine learning-based analysis of magnetic resonance radiomics for the classification of gliosarcoma and glioblastoma. *Front Oncol*. 2021;11:699789. doi:10.3389/fonc.2021.699789
7. Awadalla AS, Al Essa AM, Al Ahmadi HH, et al. Gliosarcoma case report and review of the literature. *Pan Afr Med J*. 2020;35:26. doi:10.11604/pamj.2020.35.26.17577
8. Doddamani RS, Meena RK, Selvam MM, et al. Intraventricular gliosarcomas: literature review and a case description. *World Neurosurg*. 2016;90:707.e5–707.e12. doi:10.1016/j.wneu.2016.03.033
9. Li J, Zhao YH, Tian SF, et al. Genetic alteration and clonal evolution of primary glioblastoma into secondary gliosarcoma. *CNS Neurosci Ther*. 2021;27(12):1483–1492. doi:10.1111/cns.13740
10. Ma R, Alexe DM, Pereira EA. Primary gliosarcoma: epidemiology, clinical presentation, management, and survival [published correction appears in J Neurosurg Sci. 2020 Oct;64(5):498]. *J Neurosurg Sci*. 2020;64(4):341–346. doi:10.23736/S0390-5616.17.04077-2
11. Din NU, Ishtiaq H, Rahim S, et al. Gliosarcoma in patients under 20 years of age. A clinicopathologic study of 11 cases and detailed review of the literature. *BMC Pediatr*. 2021;21(1):101. doi:10.1186/s12887-021-02556-9
12. de Macedo Filho LJM, Barreto EG, Martins PLB, et al. IDH1-mutant primary intraventricular gliosarcoma: case report and systematic review of a rare location and molecular profile. *Surg Neurol Int*. 2020;11:372. doi:10.25259/SNI_586_2020
13. Meloni M, Serra S, Bellisano G, et al. Primary gliosarcoma of the cerebellum in a young pregnant woman: management challenges and immunohistochemical features. *Case Rep Surg*. 2019;2019:7105361. doi:10.1155/2019/7105361
14. Sugita Y, Terasaki M, Tanigawa K, et al. Gliosarcomas arising from the pineal gland region: uncommon localization and rare tumors. *Neuropathology*. 2016;36(1):56–63. doi:10.1111/neup.12226
15. Prado RMA, Tamura BP, Gomez GD. Optic pathway gliosarcoma: a very rare location for a rare disease. *Radiol Case Rep*. 2021;16(7):1665–1668. doi:10.1016/j.radcr.2021.04.001
16. Shieh LT, Guo HR, Chang YK, et al. Clinical implications of multiple glioblastomas: an analysis of prognostic factors and survival to distinguish from their single counterparts. *J Formos Med Assoc*. 2020;119(3):728–734. doi:10.1016/j.jfma.2019.08.024
17. Zhang Y, Ma JP, Weng JC, et al. The clinical, radiological, and immunohistochemical characteristics and outcomes of primary intracranial gliosarcoma: a retrospective single-centre study. *Neurosurg Rev*. 2021;44(2):1003–1015. doi:10.1007/s10143-020-01285-4
18. Meyer RM, Miller CA, Coughlin DJ, et al. Glioblastoma recurrence, progression, and dissemination as a purely subdural gliosarcoma. *J Neurooncol*. 2017;132(3):521–522. doi:10.1007/s11060-017-2397-9

19. Lee J, Rodriguez F, Ali SZ. Metastatic gliosarcoma: cytopathologic characteristics with histopathologic correlations. *Acta Cytol*. 2016;60(5):490–494. doi:10.1159/000448509
20. Saadeh F, El Iskandarani S, Najjar M, et al. Prognosis and management of gliosarcoma patients: a review of literature. *Clin Neurol Neurosurg*. 2019;182:98–103. doi:10.1016/j.clineuro.2019.05.008
21. Noch EK, Sait SF, Farooq S, et al. A case series of extraneural metastatic glioblastoma at Memorial Sloan Kettering Cancer Center. *Neurooncol Pract*. 2021;8(3):325–336. doi:10.1093/nop/npaa083
22. Mittal N, Tayal S. Advance computer analysis of magnetic resonance imaging (MRI) for early brain tumor detection. *Int J Neurosci*. 2021;131(6):555–570. doi:10.1080/00207454.2020.1750390
23. Zhang BY, Chen H, Geng DY, et al. Computed tomography and magnetic resonance features of gliosarcoma: a study of 54 cases. *J Comput Assist Tomogr*. 2011;35(6):667–673. doi:10.1097/RCT.0b013e3182331128
24. Sampaio L, Linhares P, Fonseca J. Detailed magnetic resonance imaging features of a case series of primary gliosarcoma. *Neuroradiol J*. 2017;30(6):546–553. doi:10.1177/1971400917715879
25. Fukuda A, Queiroz LS, Reis F. Gliosarcomas: magnetic resonance imaging findings. *Arq Neuropsiquiatr*. 2020;78(2):112–120. doi:10.1590/0004-282x20190158
26. Kiang KM, Chan AA, Leung GK. Secondary gliosarcoma: the clinicopathological features and the development of a patient-derived xenograft model of gliosarcoma. *BMC Cancer*. 2021;21(1):265. doi:10.1186/s12885-021-08008-y
27. Romero-Rojas AE, Diaz-Perez JA, Ariza-Serrano LM, Amaro D, Lozano-Castillo A. Primary gliosarcoma of the brain: radiologic and histopathologic features. *Neuroradiol J*. 2013;26(6):639–648. doi:10.1177/197140091302600606
28. Farche MK, Fachinetti NO, da Silva LR, et al. Revisiting the use of proton magnetic resonance spectroscopy in distinguishing between primary and secondary malignant tumors of the central nervous system. *Neuroradiol J*. 2022;35(5):619–626. doi:10.1177/19714009221083145
29. Server A, Josefsen R, Kulle B, et al. Proton magnetic resonance spectroscopy in the distinction of high-grade cerebral gliomas from single metastatic brain tumors. *Acta Radiol*. 2010;51(3):316–325. doi:10.3109/02841850903482901
30. Matsumura A, Isobe T, Takano S, et al. Non-invasive quantification of lactate by proton MR spectroscopy and its clinical applications. *Clin Neurol Neurosurg*. 2005;107(5) :379–384. doi:10.1016/j.clineuro.2004.10.009
31. Schwingel R, Reis F, Zanardi VA, et al. Central nervous system lymphoma: magnetic resonance imaging features at presentation. *Arq Neuro-Psiquiatr*. 2012;70(2):97–101. doi:10.1590/s0004-282x2012000200005
32. Srivastava H, Dewan A, Sharma SK, et al. Adjuvant radiation therapy and temozolomide in gliosarcoma: is it enough? Case series of seven patients. *Asian J Neurosurg*. 2018;13(2):297–301. doi:10.4103/ajns.AJNS_151_16
33. Smith DR, Wu CC, Saadatmand HJ, et al. Clinical and molecular characteristics of gliosarcoma and modern prognostic significance relative to conventional glioblastoma. *J Neurooncol*. 2018;137(2):303–311. doi:10.1007/s11060-017-2718-z
34. Chen B, Liu B, Wu C, Wang Z. Prognostic factors among single primary gliosarcoma cases: a study using Surveillance, Epidemiology, and End Results data from 1973–2013. *Cancer Med*. 2019;8(14):6233–6242. doi:10.1002/cam4.2503
35. Yoshida Y, Ide M, Fujimaki H, et al. Gliosarcoma with primitive neuronal, chondroid, osteoid and ependymal elements [published online ahead of print, 2018 Mar 5]. *Neuropathology*. 2018. doi:10.1111/neup.12461
36. Acharya UR, Hagiwara Y, Sudarshan VK, et al. Towards precision medicine: from quantitative imaging to radiomics. *J Zhejiang Univ Sci B*. 2018;19(1):6–24. doi:10.1631/jzus.B1700260